Appendix: Looking at Non-Linear Dimension Reductions as Models in the Data Space

Jayani P.G. Lakshika
Econometrics & Business Statistics, Monash University
and
Dianne Cook
Econometrics & Business Statistics, Monash University
and
Paul Harrison
MGBP, BDInstitute, Monash University
and
Michael Lydeamore
Econometrics & Business Statistics, Monash University
and
Thiyanga S. Talagala
Statistics, University of Sri Jayewardenepura

April 20, 2025

Notation	Description
n, p, k	number of observations, variables, embedding dimension, respectively
$\boldsymbol{X}, \boldsymbol{x}$	p-dimensional data (population, sample)
$\boldsymbol{y}$	k-dimensional layout
P	orthonormal basis, generating a d-*dimensional* linear projection of p-dimensional data
T	true model
g	functional mapping from p-D to k-D, especially as prescribed by NLDR
$\boldsymbol{\theta}$	(Hyper-) parameters for NLDR method
r	ranges of the embedding components
$C^{(j)}$	j-dimensional bin centers
(b_1, b_2)	number of bins in each direction
(a_1, a_2)	binwidths, distance between centroids in each direction
$(s_1, \ s_2)$	starting coordinates of the hexagonal grid
q	buffer to ensure hexgrid covers data, proportion of data range, 0-1
m	number of non-empty bins
b	number of hexagons in the grid
h	hexagonal id
l	side length
A	area

Table 1: Summary of notation for describing new methodology.

1 Computing hexagon grid configurations

Given range of embedding component, r_2, number of bins along the x-axis, b_1, and buffer proportion, q, hexagonal starting point coordinates, $s_1 = -q$, and $s_2 = -q \times r_2$. The purpose is to find width of the hexagon. a_1, and number of bins along the y-axis, b_2.
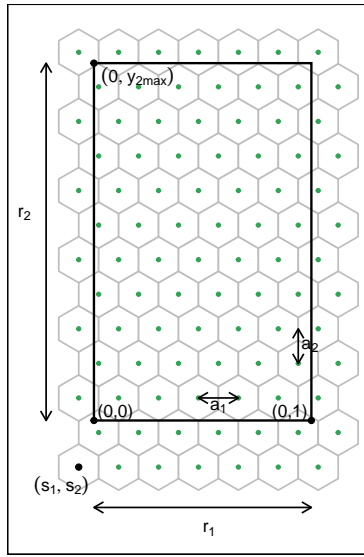
Figure 1: The components of the hexagon grid illustrating notation.

Geometric arguments give rise to the following constraints.

min a_1 s.t.

$$s_1 - \frac{a_1}{2} < 0, \tag{1}$$

$$s_1 + (b_1 - 1) \times a_1 > 1, \tag{2}$$

$$s_2 - \frac{a_2}{2} < 0, \tag{3}$$

$$s_2 + (b_2 - 1) \times a_2 > r_2. \tag{4}$$

Since a_1 and a_2 are distances,

$$a_1, a_2 > 0.$$

Also, $(s_1, s_2) \in (-0.1, -0.05)$ as these are multiplicative offsets in the negative direction.

Equation 1 can be rearranged as,

$$a_1 > 2s_1$$

which given $s_1 < 0$ and $a_1 > 0$ will *always* be true. The same logic follows for Equation 3 and substituting $a_2 = \frac{\sqrt{3}}{2}a_1$, and $s_2 = -q \times r_2$ to Equation 3 can be written as,

$$a_1 > -\frac{4}{\sqrt{3}}qr_2$$

Also, substituting $a_2 = \frac{\sqrt{3}}{2}a_1$, $s_2 = -q \times r_2$ and rearranging Equation 4 gives:

$$a_1 > \frac{2(r_2 + qr_2)}{\sqrt{3}(b_2 - 1)}. \tag{5}$$

Similarly, substituting $s_1 = -q$ Equation 2 becomes,

$$a_1 > \frac{(1 + q)}{(b_1 - 1)}. \tag{6}$$

This is a linear optimization problem. Therefore, the optimal solution must occur on a vertex. So, by setting Equation 5 equals to Equation 6 gives,

4

$$\frac{2(r_2 + qr_2)}{\sqrt{3}(b_2 - 1)} = \frac{(1 + q)}{(b_1 - 1)}.$$

After rearranging this,

$$b_2 = 1 + \frac{2r_2(b_1 - 1)}{\sqrt{3}}$$

and since b_2 should be an integer,

$$b_2 = \left\lceil 1 + \frac{2r_2(b_1 - 1)}{\sqrt{3}} \right\rceil. \tag{7}$$

Furthermore, with known b_1 and b_2, by considering Equation 2 or Equation 4 as the *binding* or *active constraint*, can compute a_1.

If Equation 2 is active, then,

$$\frac{(1 + q)}{(b_1 - 1)} < \frac{2(r_2 + qr_2)}{\sqrt{3}(b_2 - 1)}.$$

Rearranging this gives,

$$r_2 > \frac{\sqrt{3}(b_2 - 1)}{2(b_1 - 1)}.$$

Therefore, if this equality is true, then $a_1 = \frac{(1+q)}{(b_1-1)}$, otherwise, $a_1 = \frac{2r_2(1+q)}{\sqrt{3}(b_2-1)}$.

5

2 Binning the data

Points are assigned to the bin they fall into based on the nearest centroid. If a point is equidistant from multiple centroids, it is assigned to the centroid with the lowest hexagonal bin ID.
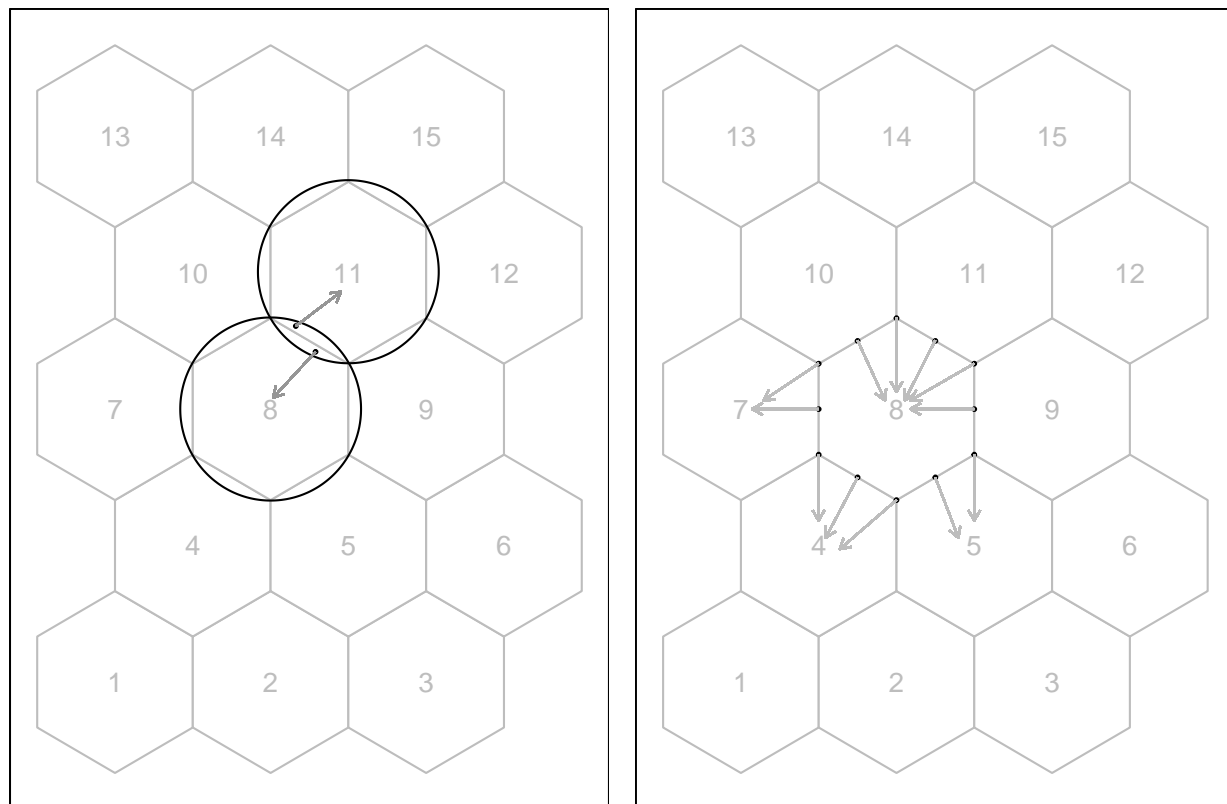

Figure 2: Binning the data. Points are assigned to the nearest centroid. If a point is equidistant from multiple centroids, assigned to the lowest centroid.

3 Area of a hexagon

The area of a hexagon is defined as $A = \frac{3\sqrt{3}}{2}l^2$, where l is the side length of the hexagon. l can be computed using a_1 and a_2.
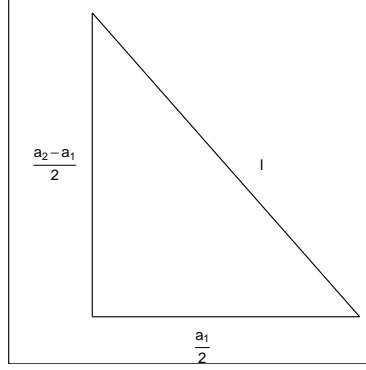

Figure 3: The components of the right triangle illustrating notation.

By applying the Pythagorean theorem, we obtain,

$$l^2 = \left(\frac{a_1}{2}\right)^2 + \left(\frac{a_2 - l}{2}\right)^2.$$

Next, rearranging the terms, we get,

$$l^2 - \left(\frac{a_2 - l}{2}\right)^2 = \left(\frac{a_1}{2}\right)^2,$$

$$\left[l - \left(\frac{a_2 - l}{2}\right)\right]\left[l + \left(\frac{a_2 - l}{2}\right)\right] = \left(\frac{a_1}{2}\right)^2,$$

$$3l^2 + 2a_2 l - (a_1^2 + a_2^2) = 0.$$

Finally, by solving the quadratic equation, we compute,

$$l = \frac{-2a_2 \pm \sqrt{4a_2^2 - 24[-(a_1^2 + a_2^2)]}}{6},$$

$$l = \frac{-a_2 \pm \sqrt{a_2^2 - 6[-(a_1^2 + a_2^2)]}}{3},$$

where $l > 0$.

3.1 Single-cell gene expression

3.1.1 Comparison with results of scDEED recommendations

As we were writing this paper Xia et al. (2023) appeared proposing a new method called scDEED helping to assess the validity of a 2-D embedding. scDEED calculates a reliability score for each cell embedding based on the similarity between the cell's 2-D embedding neighbors and its neighbors prior to embedding. A low reliability score suggests a dubious embedding. It can help in the deciding on optimal hyper-parameters. Here we illustrate how our method compares with the results from scDEED.

Following the process in Xia et al. (2023) again using the Human Peripheral Blood Mononuclear Cells (PBMC) data. Note that Xia et al. (2023) uses a different subset from the PBMC dataset used by Chen et al. (2024), which contains $31,021$ cells including cell type labels, and the gene expression levels were in the unit of log-transformed UMI count per $10,000$. They focused on three sequencing methods (inDrops, DropSeq, and SeqWell) and four common cell types Cytotoxic T cell, CD4+T cell, CD14+ Monocyte, and B cell.

For illustration purposes, we only selected cells generated with inDrops ($n = 5858$ cells) and UMAP cell embeddings. Also, Xia et al. (2023) used first 9 principal components to

generate the UMAP. The objective is to assess the optimized layout by scDEED, and if it does not accurately represent the three clusters with small separations of the PBMC dataset, then select a reasonable 2-D layout.

The layout a (Figure 4) is generated from the hyper-parameters suggested by Chen et al. (2024), and the layout b (Figure 4) is with suggested hyper-parameters by scDEED to be more accurate. The layout a and b contain 46 and 15 dubious cells respectively.

The log MSE vs binwidth (a_1) plot (Figure 4) illustrates that our approach would suggest that scDEED is correct here, that layout b is more accurately reflecting the cluster structure in the PBMC data.
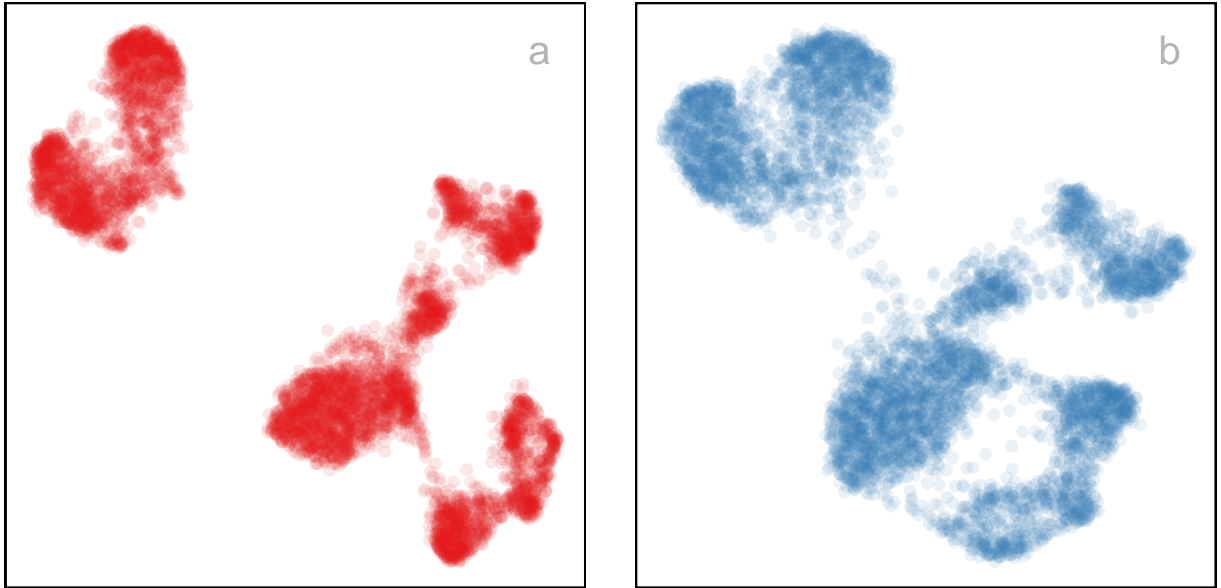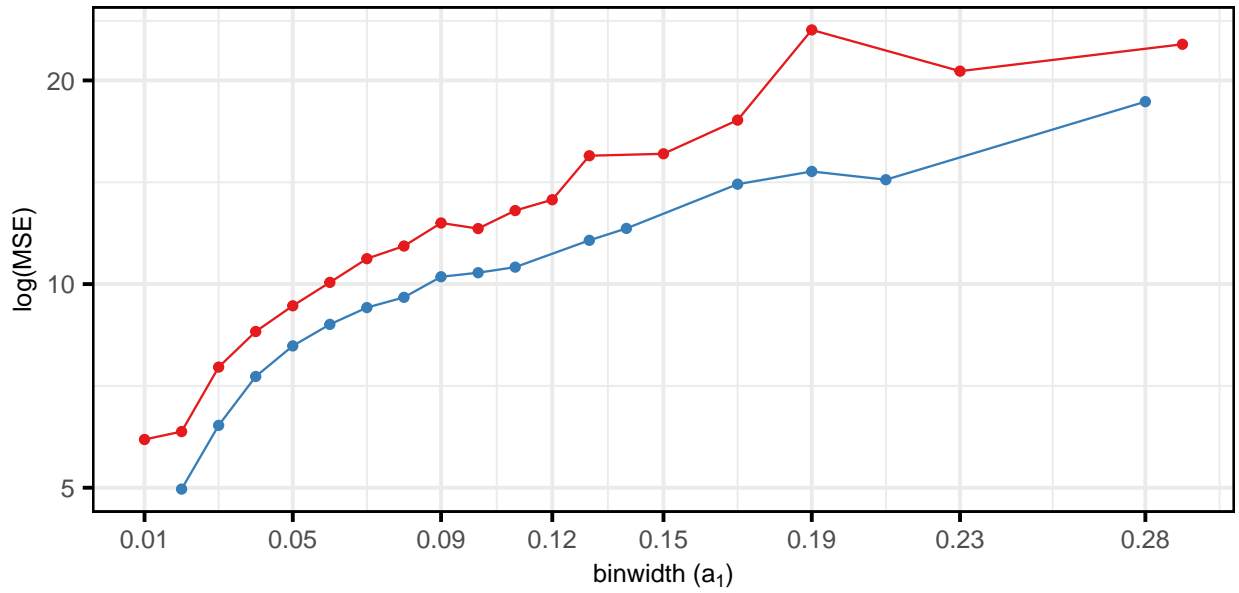
Figure 4: Assessing which of the two UMAP layouts with different hyper-parameter settings (n_neighbors: 30, min_dist: 0.3 (red); n_neighbors: 80, min_dist: 0.5 (blue)) on the PBMC data is the better representation using MSE for varying binwidth (a_1). Colour used for the lines and points in the top plot and in the scatterplots represents UMAP layout (a, b). Of the two, layout b is optimal across all binwidths making it the best choice.
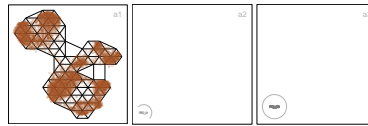

Figure 5: Model in 2-D, on the layout a, and two views of the fit in projections from 50-D, for the PBMC data ($n = 5858$ and $p = 50$). Layout shows close clusters. In 50-D, the data shows

References

Chen, Z., Wang, C., Huang, S., Shi, Y. & Xi, R. (2024), 'Directly selecting cell-type marker genes for single-cell clustering analyses', *Cell Reports Methods* **4**(7), 100810. https://www.sciencedirect.com/science/article/pii/S2667237524001735.

Xia, L., Lee, C. & Li, J. J. (2023), 'scdeed: A statistical method for detecting dubious 2d single-cell embeddings', *bioRxiv* . https://www.biorxiv.org/content/early/2023/04/25/2023.04.21.537839.